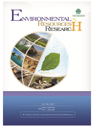

Environmental Resources Research
Vol. 8, No. 2, 2020

GUASNR

Spatiotemporal prediction of chlorophyll-*a* concentration in the Caspian Sea using logistic regression and Markov chain

F. Moëzzi[1], H. Poorbagher[2*], S. Eagderi[2], J. Feghhi[3]
[1]PhD student, Department of Fisheries, Faculty of Natural Resources, University of Tehran, Karaj, Iran
[2]Associate Professor, Department of Fisheries, Faculty of Natural Resources, University of Tehran, Karaj, Iran
[3]Professor, Department of Forestry and Forest Economics, Faculty of Natural Resources, University of Tehran, Karaj, Iran

Received: June 2020; Accepted: September 2020

Abstract
Primary production is the most important functional feature of terrestrial and aquatic ecosystems affecting many processes. In this study, we integrated logistic regression and Markov chain to predict chlorophyll-*a* (chl-*a*) concentration as an index of primary production in the Caspian Sea. We categorized the continuous variable, chl-*a*, using quantile method for analysis and prediction. Remotely-sensed data of chl-*a* and nine environmental variables were downloaded from MODIS dataset for the years 2013 and 2016. The level of chl-*a* in 2019 was predicted across the Caspian Sea. Chl-*a* data was divided into three distinct levels (i.e. low, medium and high) based on 0.33 and 0.67 quantiles, and a logistic regression model was used based on transition between the levels of chl-*a* between 2013 and 2016, and between 2016 and 2019. The Markov chain modelling indicated an increasing trend in chl-*a* levels (low to medium, low to high, medium to high) for some parts of the Caspian Sea, and also a stable condition for other parts including transition from medium to medium, high to high had the highest transition probabilities for both periods. From 2013 to 2019, the calculated areas of the pixels having low levels of chl-*a* decreased and there were considerable increases in the areas with medium and high chl-*a* levels. Accordingly, the chl-*a* level in the Caspian Sea at 2019 was predicted to be higher than those of the previous years, especially in the middle and southern parts of the Sea.

Keywords: Primary production, Caspian Sea, Simulation, Spatiotemporal, Modelling

Introduction
The production capacity of the marine ecosystems is largely impacted by environmental changes (Sissenwine and Murawski, 2004) which finally influence the available fisheries resources. Detecting physical and biological variables influencing the productivity along with a simulation of their future probable status is useful to adopt appropriate management strategies (Roessig et al., 2004; Wilsey et al., 2013). The remotely-sensed data have been increasingly used for assessing trends of environmental variables in the aquatic realms over the last decades. Satellite data are accurate, low-cost and easily-accessible and as such are being increasingly used in modelling studies (Guisan and Zimmermann, 2000). Such data provide reliable information about the productivity of aquatic ecosystems on a global scale (Behrenfeld et al., 2006) enabling zonation and mapping of aquatic areas for different purposes including fisheries management and defining marine protected areas (Schismenou et al., 2017). Combining remotely sensed data and different modelling approaches makes it possible to predict the trend of habitat parameters, species distribution and abundance (Razgour et al., 2011; Gschweng et al., 2012; Matawa et al., 2012).

Logistic regression is one of the statistical models that relate continuous independent variables to binary dependent variables. Logistic regression can be used to predict the probability of an event recorded

* Corresponding author: poorbagher@ut.ac.ir

as presence or absence. Markov Chain (MC) is a modelling approach that has been used in different fields including land use or land cover alteration, urban expansion, wetland, plant growth, watershed management, site selection and coastal zone management (Ghosh et al., 2017). A MC model is a stochastic process that computes probabilities of changes from one state to another over consecutive time points. A MC model can only predict the magnitude of changes between different states in time intervals (Boerner et al., 1996), however, it is not able to find the distribution of changes over spatial extents (Ghosh et al., 2017). For this purpose, an allocation process has to be integrated into a MC model to allocate the values predicted by the model. For example, cellular automata modelling has been frequently used to alleviate this problem (Yassemi et al., 2008; Li et al., 2010; Liu et al., 2010; Jokar Arsanjani et al., 2011). It has been suggested that the integration of these two modelling approaches improves the reliability of final predictions (Kamusoko et al., 2009; Guan et al., 2011; Sang et al., 2011). Due to the simplicity of computations for pixel-based data, a combination of logistic regression and MC modelling is a useful technique in studies that simulate geographical dynamic systems.

The Caspian Sea is the largest inland water ecosystem in the world being subjected to numerous natural and anthropogenic changes including climate change, sea level fluctuations (Arpe et al., 2000; Renssen et al. 2007; Ibrayev et al., 2010), invasion of exotic species (Kideys et al., 2008; Roohi et al., 2010), eutrophication (Nasrollahzadeh et al., 2008) and industrial waste contamination (de Mora et al., 2004; Askarova and Mussagalliyeva, 2014). The Sea supports commercial fish stocks, most of them being planktivorous pelagic fish species (Kideys et al., 2008). Changes in planktonic primary production is an important factor affecting fluctuations of fish stocks (Chassot et al., 2010). Hence, investigating the alteration of primary production over time and space could be useful for the management of fishery resources. The present study aimed to use remotely-sensed environmental data and an integrated approach of logistic regression and MC modelling to examine the relationships between chl-*a* concentration and some environmental variables (as driving forces) to find probabilities of changes in chl-*a* concentrations from 2013 to 2016. Finally, we also pursued prediction of chl-*a* concentration across the Caspian Sea using an allocation algorithm. The flowchart of the modelling steps is presented in Figure 1. Results of this study may be useful to the fishery and environmental managers.

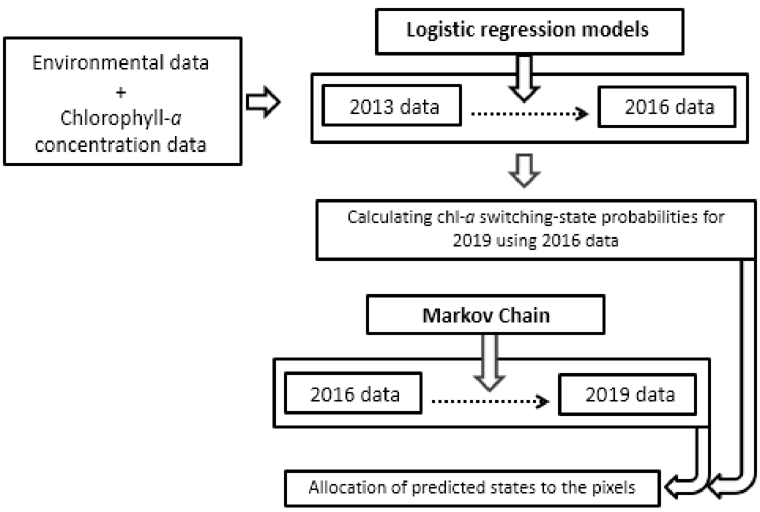

Figure 1. Flowchart of the modelling steps.

Materials and Methods

Data sets

Environmental data of the Caspian Sea were downloaded from the website of the MODIS project, NASA (http://modis.gsfc.nasa.gov). Environmental variables comprised remote sensing reflectance at 645 nm (r645, sr^{-1}) being considered as water turbidity (Chen et al., 2007), aerosol angstrom coefficient (443 to 965 nm), aerosol optical thickness at 869 nm, organic and inorganic particulate carbon (mol m^{-3}), photo-synthetically active radiation (Einstein m^{-2} day^{-1}), remote sensing reflectance at 443 nm (m^{-1}) as light absorption by phytoplankton, day- and night-time sea surface temperature (°C) and chl-*a* concentration (mg m^{-3}) as an index of primary production. Annually-averaged data of the variables were in the NetCDF format and were converted to raster format using the raster package in R (version 3.5.1). Two raster layers are needed to model temporal changes using MC. Therefore, environmental data of the years 2013 and 2016 were used for predicting chl-*a* of the year 2019. Chl-*a* data (years 2013 and 2016) were converted to ordinal data levels using their 0.33 and 0.67 quantiles: low (chl-*a* < 1.936 mg m^{-3}), medium (1.936 mg m^{-3} ≤ chl-*a* < 3.808 mg m^{-3}) and high (3.808 mg m^{-3} ≤ chl-*a*).

Logistic Regression

Based on the classification of chl-*a* into the low, medium and high levels, nine transitional states were defined for each pixel in the Caspian Sea from 2013 to 2016. For each transitional state of the pixels, one logistic regression was fitted. Environmental data and chl-*a* concentration were the predictors and the dependent variable, respectively. Hence, the nine logistic regressions predicted the probability of the specific transitional states for each pixel. Using the regression models and environmental data of the year 2016, the probability of each pixel to have a low, medium or high level chl-*a* concentration was calculated. In regression modelling, 70 and 30% of data were randomly selected as training and test data, respectively. Monte Carlo cross-validation approach was used to avoid over-fitting, where modelling was performed 25 times and each time 75% of the selected data were used to fit the model and the rest were used to test the final model. The relative operating characteristic (ROC) method was used to assess the performance of the fitted models. All of the regression modellings was conducted using the package caret in R (Kuhn and Johnson, 2013).

Prediction

The approach of the present study was mainly based on Jokar Arsanjani et al. (2013) who integrated MC and logistic regression. The predicted values were allocated to the pixels using cellular automata. We allocated the predicted values to the pixels based on the highest probability of a specific transitional state as calculated by the logistic regression.

The MC model

The nine transitional states between chl-*a* levels were found by counting the pixels belonging to each state from 2013 to 2016 and resulted in a transition matrix (3 × 3). The states of the pixels (in 2019) were predicted using the transition matrix calculated by the markovchain package in R. Finally, the counts of the pixels belonging to each chl-*a* concentration level were calculated for 2019.

Allocation of predicted data to each pixel

The counts of the cells belonged to each level of chl-*a* in 2019 (low, medium and high) were obtained from the MC modelling, however, the MC modelling was unable to detect the future (2019) level of chl-*a* in each pixel. The calculated probabilities from logistic regressions were used to determine the final condition of the pixels in 2019. For example, the low level of chl-*a* was allocated to the pixels of the Caspian Sea with the highest probability of having a low chl-*a* level in 2019. This method was conducted for other eight transitional states over the Caspian Sea.

Results and Discussion

Chl-a concentration classification

Figure 2 shows the box-plot of chl-*a* concentration levels. Converting chlorophyll-a concentration (chl-*a*; mg.m^{-3}) into low, medium and high classes was conducted using 0.33 and 0.67 quantiles. The chl-*a* values of 0.0 to 1.936 (mg m^{-3}) were considered as low level, 1.936 to 3.808 (mg m^{-3}) as medium level, and concentrations higher than 3.808 (mg m^{-3}) as high level.

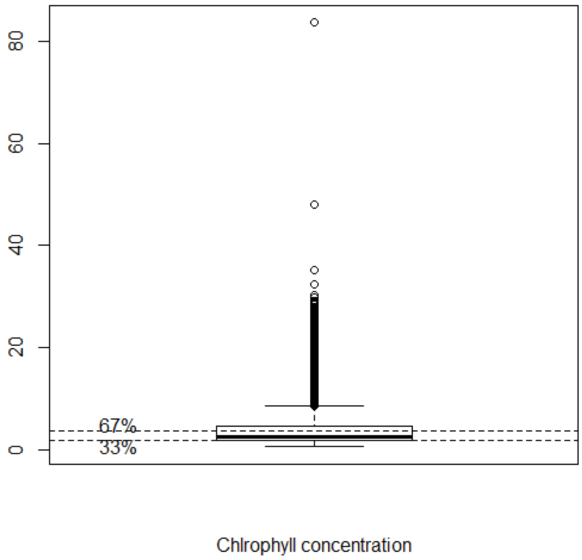

Figure 2. Box-plot of chl-*a* concentration for the years 2013 and 2016, and their 0.33 and 0.67 quantiles. Dots on the plot show outliers.

Logistic regression

The logistic regression models are presented in Table 1. The fitted regression models had ROC values > 0.5. The lowest ROC belonged to the transitional state of high to medium (0.514), and the highest value belonged to the state no-change (low to low; 0.950). All ROC values of the test data were > 0.77.

Table 1. The calculated parameters for the logistic regressions related to each transitional state between chl-*a* concentrations and ROC values for the data for model calibration and testing

Transitional chl-*a* concentration state		Sensitivity	Specificity	ROC (calibration)	ROC (testing)	Absolute difference of ROC values
Form (2013)	To (2016)					
Low	Low	0.637	0.983	0.950	0.952	0.002
Low	Medium	0.772	0.763	0.862	0.876	0.014
Low	High	0.157	0.976	0.870	0.869	0.001
Medium	Low	0.080	0.998	0.862	0.829	0.033
Medium	Medium	0.074	0.983	0.764	0.773	0.009
Medium	High	0.038	0.995	0.849	0.836	0.013
High	Low	Impossible to fit a model due to limited data				
High	Medium	0.240	0.999	0.514	0.818	0.304
High	High	0.908	0.990	0.996	0.984	0.012

MC modelling

The transition probability matrix calculated based on the data of the years 2013 and 2016 (Table 2), showed that part of the Caspian Sea remained unchanged, at the state of high chl-*a* concentration (H-H; > 3.808 mg m^{-3}) with the highest probability. The transition from low to medium (L-M) levels and remaining in the medium state (M-M) were the next high-probability states. The transition states from medium and high levels to low and medium levels (M-L; H-M), respectively, had the lowest probabilities.

Table 2. The transition probability matrix based on the pixel counts for each level of chl-*a* level (low, medium and high) from 2013 to 2016

		2016		
		Low	Medium	High
	Low	0.188	0.638	0.174
2013	Medium	0.007	0.590	0.403
	High	0.001	0.024	0.975

The transition probability matrix predicted by the MC model (Table 3) indicated that the areas of the Caspian Sea with high chl-*a* levels (*i.e.*, high primary productivity) will be maintained at the same state in 2019. The increasing transitional states (i.e. transition from low and medium to medium and high levels, respectively; L-M; M-H) were the most probable transitional states.

Table 3. The transition probability matrix of the chl-*a* level predicted by Markov Chain (MC) model from 2016 to 2019

		2019		
		Low	Medium	High
	Low	0.040	0.500	0.459
2016	Medium	0.006	0.362	0.631
	High	0.001	0.038	0.960

There were several missing values in the satellite data for some of the environmental predictors. Hence, it was not possible to calculate the probability of a given transitional state by a logistic regression model in some pixels across the Caspian Sea. These pixels were mainly located in the north of the Sea (Figure 3). The probability of each transitional state of chl-*a* level between 2016 and 2019 showed that a small area of the Caspian Sea (the eastern coast) will continue to have low levels of chl-*a* in 2019 (Figure 3). The middle parts (mainly offshore areas) of the Sea have the potential to increase their chl-*a* level from low to medium and high levels (Figure 3). There was not a high probability for other transitional states in chl-*a* levels and only, the northern parts of the Caspian Sea showed a high probability for remaining in the high level of chl-*a* (Figure 3).

The areas of the pixels estimated to have different chl-*a* levels in the Caspian Sea are presented in Table 4. These areas were calculated based on the number of pixels belonging to each level of chl-*a* concentration. Since there were missing values in the raster layers of the satellite data, the total area of the Caspian Sea was not fully covered over the years. Therefore, in addition to the area values, the percentage of the pixels for each chl-*a* level is presented in Table 4. Compared to 2013, a large area of the Caspian Sea was shown to have medium and high chl-*a* level in 2019 indicating an increase in trophic state of the Sea.

Table 4. Estimated area (km^2; %) of the pixels belonging to different chl-*a* levels for the years 2013, 2106 and 2019. Due to the missing values in the satellite data, the total area of the Sea is different over the years

Chl-*a* level	Low		Medium		High	
year	km^2	%	km^2	%	km^2	%
2013	219352.06	57	78380.15	20	89701.46	23
2016	43749.14	11	192854.63	49	158101.52	40
2019	43997.51	13	187362.08	55	109145.35	32

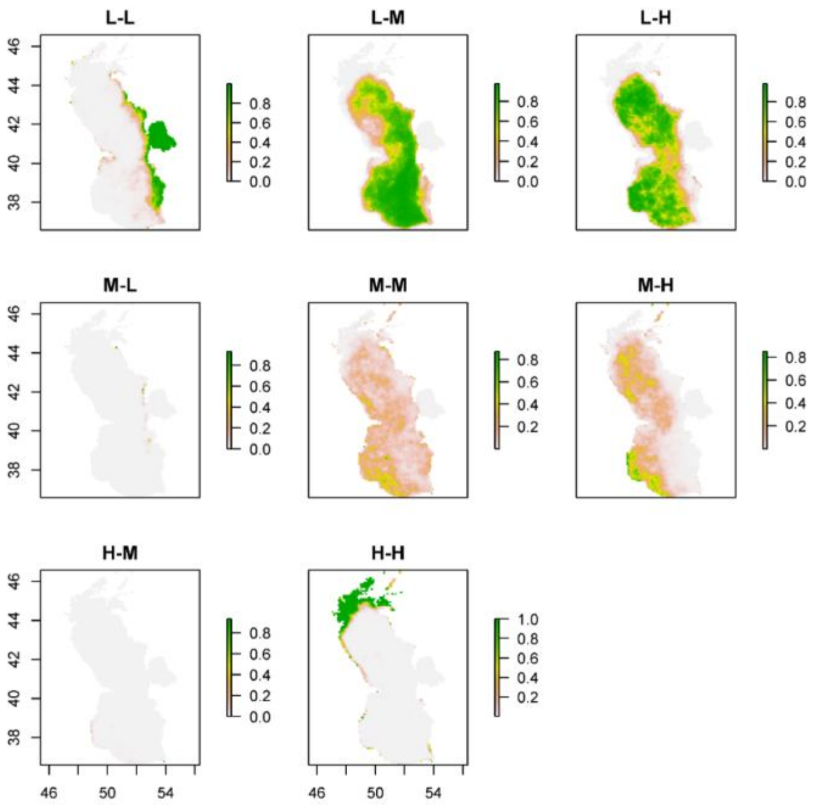

Figure 3. The calculated probability for the transition between chl-*a* levels (Low: L; medium: M; High: H) from 2016 to 2019. Because of missing values in environmental variables, the fitted logistic regressions estimated no probability for the northern parts of the Caspian Sea.

The map of chl-*a* level for the year 2013 (Figure 4) showed that the Kara-Bogaz-Gol Bay, and the major parts of the eastern coast and most offshore areas of the Sea had low levels of chl-*a*. The waters near the Iranian coasts, Turkmenistan and Azerbaijan had medium levels of chl-*a*. The highest levels of chl-*a* were found in inshore waters of Kazakhstan, Russia, Iran and some points in Azerbaijan and Turkmenistan coasts. The map of chl-*a* for 2016 showed that most parts of the Caspian Sea had a medium level of chl-*a* (Figure 5). As before, the Kara-Bogaz-Gol Bay and some parts of Turkmenistan and parts of the Iranian offshore waters had a low chl-*a* level. The coastal waters of Iran, Azerbaijan, Russia and Kazakhstan had the highest chl-*a* concentration. The predicted chl-*a* concentration for 2019 showed that low levels of chl-*a* in the Caspian Sea will be limited to the offshore areas of the middle and northern parts of the Sea (Figure 6). The greatest area of the Sea was shown to have a medium level of chl-*a* in 2019. The high chl-*a* level belonged to the coasts of Turkmenistan and Kara-Bogaz-Gol Bay. As with prior years, the waters of Russia and Kazakhstan would have high levels of chl-*a*. Also, coastal waters of Azerbaijan would have high levels of chl-*a*. The highest chl-*a* level in the Iranian waters would occur in the southeast regions of the Sea.

During the past years, multiple modelling methods have been combined to find spatial and temporal interactions between components of dynamic systems and utilizing these relationships over time and space to predict upcoming situations of these systems (Abolhasani et al., 2016; Aburas et al., 2016; Azari et al., 2016; Berberoğlu et al., 2016; Chen et al., 2016; Ku, 2016; Omrani et al., 2017; Shafizadeh-Moghadam et al., 2017). In the present study, we integrated logistic regression and Markov Chain to examine the relationship of chl-*a* concentrations of the Caspian Sea with remotely-sensed variables in 2013 and 2016, and finally predicting spatial changes of chl-*a* in 2019. This technique is not new and has been used to predict land surface alterations, such as urban expansion and land-use change (Jokar Arsanjani et al., 2011; Jokar Arsanjani et al., 2013; Ku, 2016; Palmate et al., 2017). However, the approach taken here to combine these modelling methods has not been used to predict changes of a given parameter over water bodies. The Markov chain model used the calculated probabilities of transitional states to quantify the extent of alterations over the whole area of the Caspian Sea based on the transition probability matrix. This matrix displayed the relative frequencies of transitional states at a certain time period (Cabral and Zamyatin, 2009). The calculated transition probabilities from 2013 to 2016 indicated that there was a high potential for the Caspian Sea to sustain the medium to a high level of chl-*a*. In contrast, decreasing from high or medium levels of chl-*a* to low levels had a low probability. Such prediction may be expected because studies regarding the eutrophic status of the Caspian Sea is not promising (Nasrollahzadeh *et al.*, 2008; Shahrban and Etemad-Shahidi, 2010). Allocation of the predicted state to each pixel of a map is the final step in the preparation of the predicted map. The cellular automata have been used to allocate the predicted condition of pixels (Jokar Arsanjani et al., 2011). In our study, the allocation process was based on the highest probability of a pixel to have a specific transitional state. This method; while having the advantage of requiring no rule, in contrast to cellular automata, was very time-consuming. A proper algorithm may alleviate this problem.

Due to incomplete coverage of satellite data for the predictor variables, the logistic regression failed to calculate the transitional probabilities of the northern parts of the Sea. However, the major part of the Sea had the required data for modelling. The predicted chl-*a* level (for 2019) shows a lot of variability compared with those of 2016. Changes in the environmental conditions such as depth (Longhurst, 1995; Kopelevich et al., 2004), pycnocline establishment in deep waters (Leonov, 2002) and discharges of the Volga River into the northern area (Leonov, 2002), have been considered as an explanation for different chl-*a* concentration in the Sea.

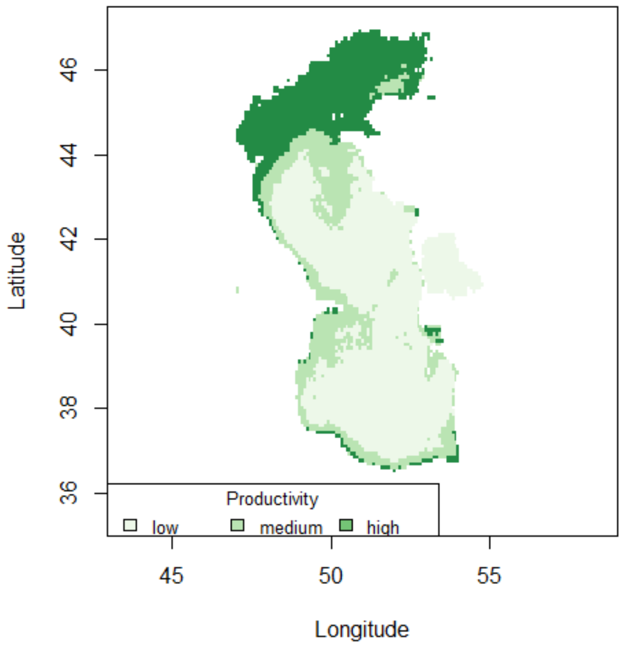

Figure 4. Map of chl-*a* level in the Caspian Sea for the year 2013.

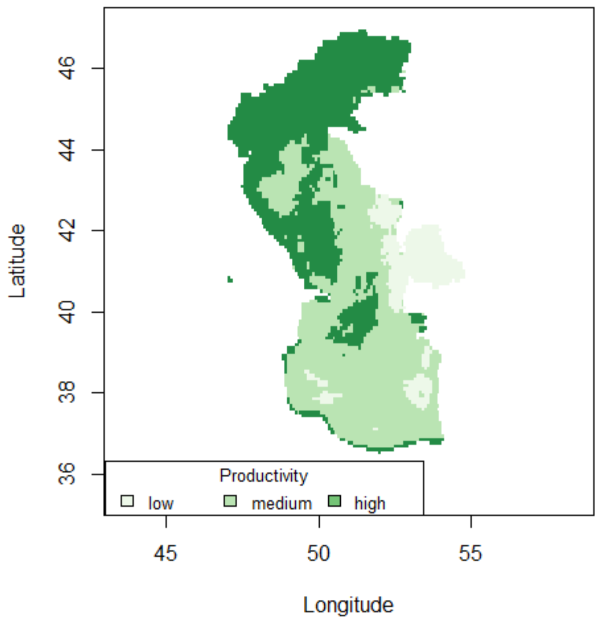

Figure 5. Map of chl-a level in the Caspian Sea for the year 2016.

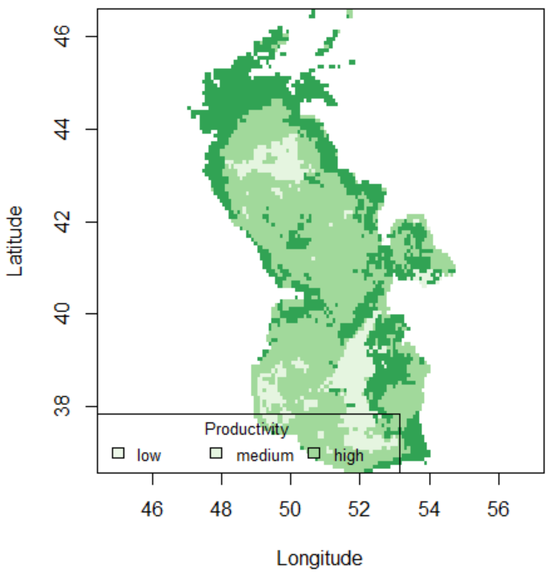

Figure 6. Map of predicted chl-*a* level of the Caspian Sea for the year 2019. Due to the lack of data for some environmental variables, chl-*a* level was not predicted for the northern parts of the Caspian Sea.

Conclusion

An approach integrating two modelling techniques including logistic regression and Markov Chain was used in this study to predict alteration of chl-*a* concentrations (as an index of primary production) over time and space in the Caspian Sea using remotely sensed data. This approach produced projections on the primary production in 2019 based on the states in the last years. Our results indicate that the Caspian Sea will face high productivity over nearly the whole of its realm. The lack of full coverage of satellite data, especially for the northern boundaries of the Caspian Sea led to an incomplete extent of predicted range at the final time point.

References

Abolhasani, S., Taleai, M., Karimi, M. and Rezaee Node, A. 2016. Simulating urban growth under planning policies through parcel-based cellular automata (ParCA) model. International Journal of Geographical Information Science. 30(11), 2276-2301.

Aburas, M.M., Ho, Y.M., Ramli, M.F. and Ash'aari, Z.H. 2016. The simulation and prediction of spatio-temporal urban growth trends using cellular automata models: A review. International Journal of Applied Earth Observation and Geoinformation. 52, 380-389.

Arpe, K., Bengtsson, L., Golitsyn, G.S., Mokhov, I.I., Semenov, V.A. and Sporyshev, P.V., 2000. Connection between Caspian Sea level variability and ENSO. Geophysical Research Letters. 27(17), 2693-2696.

Askarova, M.A. and Mussagaliyeva, A.N. 2014. The ecological situation in contaminated areas of oil and gas exploration in Atyrau Region. Procedia-Social and Behavioral Sciences. 120, 455-459.

Azari, M., Tayyebi, A., Helbich, M. and Reveshty, M.A., 2016. Integrating cellular automata, artificial neural network, and fuzzy set theory to simulate threatened orchards: application to Maragheh, Iran. GIScience and Remote Sensing. 53(2), 183-205.

Behrenfeld, M.J., O'Malley, R.T., Siegel, D.A., McClain, C.R., Sarmiento, J.L., Feldman, G.C., Milligan, A.J., Falkowski, P.G., Letelier, R.M. and Boss, E.S. 2006. Climate-driven trends in contemporary ocean productivity. Nature. 444(7120), p.752.

Berberoğlu, S., Akın, A. and Clarke, K.C. 2016. Cellular automata modeling approaches to forecast urban growth for adana, Turkey: A comparative approach. Landscape and Urban Planning. 153, 11-27.

Boerner, R.E., DeMers, M.N., Simpson, J.W., Artigas, F.J., Silva, A. and Berns, L.A. 1996. Markov models of inertia and dynamism on two contiguous Ohio landscapes. Geographical Analysis. 28(1), 56-66.

Cabral, P. and Zamyatin, A. 2009. Markov processes in modeling land use and land cover changes in Sintra-Cascais, Portugal. Dyna. 76(158), 191-198.

Chassot, E., Bonhommeau, S., Dulvy, N.K., Mélin, F., Watson, R., Gascuel, D. and Le Pape, O. 2010. Global marine primary production constrains fisheries catches. Ecology Letters. 13(4), 495-505.

Chen, Z., C., Hu, F., Muller-Karger. 2007. Monitoring turbidity in Tampa Bay using MODIS/Aqua 250-m imagery. Remote sensing of Environment. 109(2), 207-220.

Chen, Y., Li, X., Liu, X., Ai, B. and Li, S. 2016. Capturing the varying effects of driving forces over time for the simulation of urban growth by using survival analysis and cellular automata. Landscape and Urban Planning. 152, 59-71.

Ghosh, P., Mukhopadhyay, A., Chanda, A., Mondal, P., Akhand, A., Mukherjee, S., Nayak, S.K., Ghosh, S., Mitra, D., Ghosh, T. and Hazra, S. 2017. Application of Cellular automata and Markov-chain model in geospatial environmental modeling-A review. Remote Sensing Applications: Society and Environment. 5, 64-77.

Giannoulaki, M., E. Schismenou, M.-M. Pyrounaki and Tsagarakis, K. 2014. Habitat characterization and migrations. In: Ganias, K. (ed.), Biology and Ecology of Sardines and Anchovies. CRC Press, Boca Raton, FL: 190–241

Grecian, W.J., Lane, J.V., Michelot, T., Wade, H.M. and Hamer, K.C. 2018. Understanding the ontogeny of foraging behaviour: insights from combining marine predator bio-logging with satellite-derived oceanography in hidden Markov models. Journal of the Royal Society Interface. 15(143), p.20180084.

Gschweng, M., Kalko, E.K., Berthold, P., Fiedler, W. and Fahr, J. 2012. Multi-temporal distribution modelling with satellite tracking data: predicting responses of a long-distance migrant to changing environmental conditions. Journal of Applied Ecology. 49(4), 803-813.

Guan, D., Li, H., Inohae, T., Su, W., Nagaie, T. and Hokao, K. 2011. Modeling urban land use change by the integration of cellular automaton and Markov model. Ecological Modelling. 222(20-22), 3761-3772.

Guisan, A. and Zimmermann, N.E. 2000. Predictive habitat distribution models in ecology. Ecological modelling, 135(2-3), 147-186.

Hu, Z. and Lo, C.P., 2007. Modeling urban growth in Atlanta using logistic regression. Computers, Environment and Urban Systems. 31(6), 667-688.

Ibrayev, R.A., Özsoy, E., Schrum, C. and Sur, H.I. 2010. Seasonal variability of the Caspian Sea three-dimensional circulation, sea level and air-sea interaction. Ocean Science. 6(1), 1-10.

Johnson, J.E. and Welch, D.J. 2009. Marine fisheries management in a changing climate: a review of vulnerability and future options. Reviews in Fisheries Science. 18(1), 106-124.

Jokar Arsanjani, J. 2011. Dynamic land use/cover change modelling: Geosimulation and multiagent-based modelling. Springer Science and Business Media.

Jokar Arsanjani, J., Kainz, W. and Mousivand, A.J. 2011. Tracking dynamic land-use change using spatially explicit Markov Chain based on cellular automata: the case of Tehran. International Journal of Image and Data Fusion. 2(4), 329-345.

Jokar Arsanjani, J., Helbich, M., Kainz, W. and Boloorani, A.D. 2013. Integration of logistic regression, Markov chain and cellular automata models to simulate urban expansion. International Journal of Applied Earth Observation and Geoinformation, 21, 265-275.

Kamusoko, C., Aniya, M., Adi, B. and Manjoro, M. 2009. Rural sustainability under threat in Zimbabwe–simulation of future land use/cover changes in the Bindura district based on the Markov-cellular automata model. Applied Geography. 29(3), 435-447.

Kideys, A.E., Roohi, A., Eker-Develi, E., Mélin, F. and Beare, D. 2008. Increased chlorophyll levels in the southern Caspian Sea following an invasion of jellyfish. International Journal of Ecology. 2008.

Kopelevich, O.V., Burenkov, V.I., Ershova, S.V., Sheberstov, S.V. and Evdoshenko, M.A. 2004. Application of SeaWiFS data for studying variability of bio-optical characteristics in the Barents, Black and Caspian Seas. Deep Sea Research Part II: Topical Studies in Oceanography. 51(10-11), 1063-1091.

Kuhn, M. and Johnson, K. 2013. Applied predictive modelling. Springer. 560p.

Ku, C.A. 2016. Incorporating spatial regression model into cellular automata for simulating land use change. Applied Geography. 69, 1-9.

Leonov, A.V. 2002. Biogenic Riverine Runoff into the Caspian Sea. Oceanology. 42(5), 651-660.

Li, X., Zhang, X., Yeh, A. and Liu, X., 2010. Parallel cellular automata for large-scale urban simulation using load-balancing techniques. International Journal of Geographical Information Science. 24(6), 803-820.

Liu, X., Li, X., Shi, X., Zhang, X. and Chen, Y. 2010. Simulating land-use dynamics under planning policies by integrating artificial immune systems with cellular automata. International Journal of Geographical Information Science. 24(5), 783-802.

Longhurst, A. 1995. Seasonal cycles of pelagic production and consumption. Progress in oceanography. 36(2), 77-167.

Matawa, F., Murwira, A. and Schmidt, K.S. 2012. Explaining elephant (*Loxodonta africana*) and buffalo (*Syncerus caffer*) spatial distribution in the Zambezi Valley using maximum entropy modelling. Ecological Modelling. 242, 189-197.

Nasrollahzadeh, H.S., Din, Z.B., Foong, S.Y. and Makhlough, A. 2008. Trophic status of the Iranian Caspian Sea based on water quality parameters and phytoplankton diversity. Continental Shelf Research. 28(9), 1153-1165.

Omrani, H., Tayyebi, A. and Pijanowski, B. 2017. Integrating the multi-label land-use concept and cellular automata with the artificial neural network-based Land Transformation Model: an integrated ML-CA-LTM modeling framework. GIScience and Remote Sensing. 54(3), 283-304.

Palmate, S.S., Pandy, A. and Mishra, S.K. 2017. Modelling spatiotemporal land dynamics for a trans-boundary river basin using integrated Cellular Automata and Markov Chain approach. Applied Geography. 82, 11-23.

Razgour, O., Hanmer, J. and Jones, G. 2011. Using multi-scale modelling to predict habitat suitability for species of conservation concern: the grey long-eared bat as a case study. Biological Conservation. 144(12), 2922-2930.

Renssen, H., Lougheed, B.C., Aerts, J.C.J.H., De Moel, H., Ward, P.J. and Kwadijk, J.C.J. 2007. Simulating long-term Caspian Sea level changes: the impact of Holocene and future climate conditions. Earth and Planetary Science Letters. 261(3-4), 685-693.

Roessig, J.M., Woodley, C.M., Cech, J.J. and Hansen, L.J. 2004. Effects of global climate change on marine and estuarine fishes and fisheries. Reviews in Fish Biology and Fisheries. 14(2), 251-275.

Roohi, A., Kideys, A.E., Sajjadi, A., Hashemian, A., Pourgholam, R., Fazli, H., Khanari, A.G. and Eker-Develi, E. 2010. Changes in biodiversity of phytoplankton, zooplankton, fishes and macrobenthos in the Southern Caspian Sea after the invasion of the ctenophore Mnemiopsis leidyi. Biological Invasions. 12(7), 2343-2361.

Sang, L., Zhang, C., Yang, J., Zhu, D. and Yun, W. 2011. Simulation of land use spatial pattern of towns and villages based on CA–Markov model. Mathematical and Computer Modelling. 54(3-4), 938-943.

Schismenou, E., Tsoukali, S., Giannoulaki, M. and Somarakis, S. 2017. Modelling small pelagic fish potential spawning habitats: eggs vs spawners and in situ vs satellite data. Hydrobiologia. 788(1), 17-32.

Shafizadeh-Moghadam, H., Asghari, A., Taleai, M., Helbich, M. and Tayyebi, A. 2017. Sensitivity analysis and accuracy assessment of the land transformation model using cellular automata. GIScience and Remote Sensing. 54(5), 639-656.

Shahrban, M. and Etemad-Shahidi, A. 2010. Classification of the Caspian Sea coastal waters based on trophic index and numerical analysis. Environmental Monitoring and Assessment. 164(1-4): 349-356.

Sissenwine, M. and Murawski, S. 2004. Moving beyond intelligent tinkering: advancing an Ecosystem Approach to Fisheries. Marine Ecology Progress Series. 274, 291-295.

Sur, H.I., Özsoy, E. and Ibrayev, R. 2000. Satellite-derived flow characteristics of the Caspian Sea. Elsevier Oceanography Series. 63, 289-297.

Wilsey, C.B., Lawler, J.J., Maurer, E.P., McKenzie, D., Townsend, P.A., Gwozdz, R., Freund, J.A., Hagmann, K. and Hutten, K.M. 2013. Tools for assessing climate impacts on fish and wildlife. Journal of Fish and Wildlife Management. 4(1), 220-241.

Yassemi, S., Dragićević, S. and Schmidt, M. 2008. Design and implementation of an integrated GIS-based cellular automata model to characterize forest fire behaviour. Ecological Modelling. 210(1-2), 71-84.

Zhu, J., Xu, J., Guo, C., Zhuo, X., Gao, Y. and Xing, S. 2016. An empirical research of marine fishery forecasting methods based on the classification model. In 2016 International Conference on Progress in Informatics and Computing (PIC) (1-7). IEEE.